

# Sequential and coordinated action of phytochromes A and B during *Arabidopsis* stem growth revealed by kinetic analysis

Brian M. Parks and Edgar P. Spalding\*

Department of Botany, University of Wisconsin, 430 Lincoln Drive, Madison, Wisconsin 53706

Communicated by Joanne Chory, The Salk Institute for Biological Studies, La Jolla, CA, October 7, 1999 (received for review August 22, 1999)

**Photoreceptor proteins of the phytochrome family mediate light-induced inhibition of stem (hypocotyl) elongation during the development of photoautotrophy in seedlings. Analyses of overt mutant phenotypes have established the importance of phytochromes A and B (phyA and phyB) in this developmental process, but kinetic information that would augment emerging molecular models of phytochrome signal transduction is absent. We have addressed this deficiency by genetically dissecting phytochrome-response kinetics, after having solved the technical issues that previously limited growth studies of small *Arabidopsis* seedlings. We show here, with resolution on the order of minutes, that phyA initiated hypocotyl growth inhibition upon the onset of continuous red light. This primary contribution of phyA began to decrease after 3 hr of irradiation, the same time at which immunochemically detectable phyA disappeared and an exclusively phyB-dependent phase of inhibition began. The sequential and coordinated actions of phyA and phyB in red light were not observed in far-red light, which inhibited growth persistently through an exclusively phyA-mediated pathway.**

Phytochromes are a family of biliprotein photoreceptors used by diverse photosynthetic organisms to monitor their light environment (1). In angiosperms, phytochrome signaling affects many aspects of development throughout the life cycle, from seed germination to flowering (2). Comparative studies of light responses in *Arabidopsis* mutants, variously deficient in four of this species' five phytochromes, is a logical and proven approach to learning the functions of each phytochrome family member (3, 4). The inhibition of hypocotyl elongation by high-irradiance red and far-red light is a photomorphogenic response that has been particularly exploited (5). Genetic studies of this important process in seedling development have identified both unique and shared functions for phyA and phyB, as well as proteins that operate downstream of one or both phytochrome types (6).

Although the standard method of measuring hypocotyl length after days of growth in light has clearly been productive, it is not capable of revealing dynamic features of how phytochrome-mediated responses develop after the onset of irradiation. Although *Arabidopsis* is the preferred plant for genetic dissections, the small size of its seedlings impedes the merging of this advantage with kinetic analyses of hypocotyl growth responses. A dark-grown (etiolated) *Arabidopsis* seedling is a mere 3 mm long when it reaches a maximum growth rate of approximately  $8\% \text{ hr}^{-1}$ . The absolute elongation rate of a 5-cm cucumber seedling growing at approximately the same relative rate is more than 10 times greater and is therefore easier to measure with high temporal resolution. Tools of the trade, such as electronic displacement transducers and time-lapsed photography, have been modified to work with *Arabidopsis* seedlings, and recently were used in a kinetic study of the rapid action of blue light. The experiments revealed that the CRY1 photoreceptor begins to affect growth only after 45–60 min of blue light, whereas a yet-unknown UVA/blue receptor initiates inhibition within 30 s (7). This unexpected result exemplifies that a close look at growth responses can add important information about mech-

anism; the present examination of responses induced by red and far-red light in wild-type and mutant *Arabidopsis* seedlings was undertaken with these results in mind.

## Materials and Methods

**Plant Material and Growing Conditions.** The Landsberg ecotype of *Arabidopsis thaliana* was used for all experiments. All phytochrome mutant lines, generously provided by Robert A. Sharrock (Montana State Univ.), were null for the particular photoreceptor type and were backcrossed five to six times into the Landsberg background (8). For growth assays, seedlings were sown and grown on an agar medium in individual capless microcentrifuge tubes or on the surface of vertical Petri plates, as previously described (7). For phytochrome extraction and detection, 50 mg of seed were evenly distributed on horizontal plates containing the same agar medium and grown in complete darkness for 3 days, yielding approximately one gram fresh weight per plate.

**Growth Assays.** The methods that we used to monitor growth of 2- to 3-day-old *Arabidopsis* seedlings have been described previously (7). Briefly, the highest-resolution growth measurements of individual seedlings were made by using an electronic displacement transducer (LVDT no. DC-E050; Lucas Control Systems, Hampton, VA), interfaced to a computerized data-acquisition system described elsewhere (9). Blue or red light was produced by filtering the light of a xenon arc through the appropriate interference filter (450 nm, 10-mm bandwidth, Corion, Holliston MA; or 670 nm, 10-mm bandwidth, Oriol, Stratford CT). Pulses were timed by a computer-controlled shutter and delivered to the seedling via a liquid light guide (9).

For longer-term growth rate analysis under continuous irradiation, a vertical plate with multiple adjacent seedlings was placed in a mount facing a computer-interfaced charge-coupled device (CCD) camera (EDC-1000N; Electrim, Princeton, NJ), equipped with a close-focus zoom lens (D52274; Edmund Scientific) achieving a resolution of  $5 \mu\text{m}$  per pixel. Seedlings were imaged throughout the experiment with radiation from infrared light-emitting diodes that does not induce photomorphogenesis in *Arabidopsis*. Actinic red (670-nm) or far-red (744-nm) illumination was supplied by a bank of light-emitting diodes (QB1310S-670-735; Quantum Devices, Barneveld, WI).

**Protein Extraction and Immunochemical Detection.** Procedures used for phytochrome purification, electrophoretic separation, and immunochemical detection were as described previously, with the following modifications (10). Frozen tissue was thawed and ground under red light at a 1-g:1.6-ml ratio in undiluted extrac-

Abbreviations: CCD, charge-coupled device; phyA, phytochrome A holoprotein; phyB, phytochrome B holoprotein; R<sub>c</sub>, continuous red light; FR<sub>c</sub>, continuous far-red light.

\*To whom reprint requests should be addressed. E-mail: spalding@factstaff.wisc.edu.

The publication costs of this article were defrayed in part by page charge payment. This article must therefore be hereby marked "advertisement" in accordance with 18 U.S.C. §1734 solely to indicate this fact.

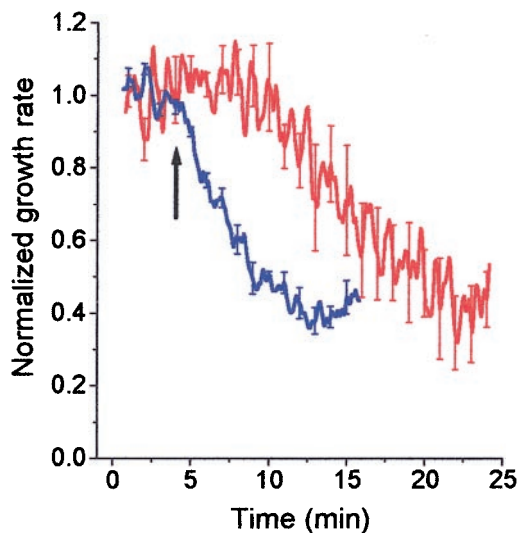


**Fig. 1.** High-resolution analysis of the growth response of *Arabidopsis* seedlings to a pulse of red light (red trace) or blue light (blue trace). Growth inhibition was induced in individual dark-grown, wild-type seedlings (<1 cm tall) by a 20-s pulse (upward arrow) of  $50 \mu\text{mol}\cdot\text{m}^{-2}\cdot\text{s}^{-1}$  monochromatic 450-nm or 670-nm light, and recorded every 5 s with an electronic displacement transducer. The rate of growth in darkness for all seedlings was approximately  $0.25 \text{ mm}\cdot\text{hr}^{-1}$ , and was normalized to the average rate of growth during the initial 4-min growth period in darkness. Each trace represents the average of five separate experiments. Error bars representing one SEM at 1-min intervals are shown. The response to blue light was published previously (7), and is represented here for comparison.

tion buffer containing all protease inhibitors, two of which (phenylmethylsulfonyl fluoride and iodoacetamide) were used at 2 mM and 10 mM, respectively. The final extraction pellet was resuspended in 3% of the original extraction volume. The solution used for blocking and antibody detection during immunodetection procedures was 0.2% milk buffer. The mAb culture supernatants that we used for the specific detection of phyA (cell line 073d) and phyB (cell line B2-A5) were a generous gift of Peter H. Quail (Univ. of California, Berkeley) and the U.S. Dept. of Agriculture Plant Gene Expression Center) and were used at 1:200 dilution. Anti-mouse IgG conjugated to alkaline phosphatase (Promega) was used as the final probe at 1:5000 dilution. Seedlings were irradiated before harvest with red or far-red light ( $250 \mu\text{mol}\cdot\text{m}^{-2}\cdot\text{s}^{-1}$ ) produced by the diode array light source described above.

## Results and Discussion

Fig. 1 shows that a pulse of either blue or red light (equal photon fluences) caused a reduction in the growth rate of etiolated *Arabidopsis* seedlings. Growth rate declined to approximately 40% of the rate in darkness, regardless of the wavelength, but the kinetics of the two responses were very different. Whereas blue light caused inhibition beginning after approximately 30 s, the red-light pulse caused no noticeable effect until approximately 8 min. Results similar to these were first obtained in other species and considered to be evidence that blue light did not inhibit hypocotyl growth by means of phytochrome (11–13), a point that has been substantiated by genetic studies, beginning with the work of Koornneef *et al.* (14). Although these data alone do not prove it, the response to red light shown in Fig. 1 is probably mediated by phytochrome. A similar experiment could be performed with various phytochrome-deficient mutants to confirm the participation of phytochrome in this response; such a test would also reveal which phytochrome types contribute to the response and when each photoreceptor acts.

Fig. 2A shows that, in wild-type seedlings, the onset of continuous red light ( $R_C$ ) at a fluence rate approaching saturation ( $250 \mu\text{mol}\cdot\text{m}^{-2}\cdot\text{s}^{-1}$ , roughly equivalent to the red component of full sunlight) caused an initial but transient growth inhibition that peaked after 15 min. This brief growth inhibition was followed by the development of a sustained phase of inhibition that produced a steady 38% inhibition after 3 hr of  $R_C$  (Fig. 2A). In contrast, double mutant seedlings lacking both phyA and phyB displayed neither the initial transient phase nor the sustained long-term inhibition during 5 hr of  $R_C$ , and were thus essentially blind to this treatment. This result is consistent with the accepted notion that phyB is primarily responsible for detecting  $R_C$  conditions, and that phyA plays a minor role.

To facilitate the genetic dissection of the response development, the growth rate time series in Fig. 2A were converted into inhibition time series  $I(t)$  according to the formula

$$I(t) = \left(1 - \frac{r(t)}{r_0}\right) \times 100\%, \quad [1]$$

where  $r(t)$  is the growth rate data set and  $r_0$  is the average dark growth rate preceding the onset of irradiation. Plots of the inhibition time series for wild-type and *phyA phyB* seedlings show directly the course of hypocotyl inhibition for the wild type (including the initial transient response marked by an asterisk) and the apparent absence of any response by the double mutant (Fig. 2B). This same analysis was performed for single mutants lacking phyA or phyB to determine the relative contributions of these photoreceptors to the  $R_C$  response of the parent wild type. The plots in Fig. 2B and C demonstrate that  $R_C$  inhibited the growth of *phyB* seedlings and the growth of wild-type seedlings with no distinguishable difference during the first 3 hr of irradiation, including the initial transient inhibition. After achieving a maximum inhibition at 3 hr, *phyB* seedlings resumed uninhibited growth, eventually exceeding the rate in darkness for a period beginning 4 hr after the onset of irradiation.

This result, as well as the complete insensitivity of the *phyA phyB* seedlings shown in Fig. 2A and B, suggests that phyA is the only photoreceptor responsible for transducing  $R_C$  into growth inhibition during the first 3 hr of irradiation. This conclusion was borne out by the response of *phyA* seedlings, which did not develop inhibition during the first 3 hr of  $R_C$ , except for the initial transient response. The occurrence of the transient response in both single mutants, and its absence in the double mutant, indicates functional overlap between phyA and phyB during this initial phase. After recovering from the initial inhibition, *phyA* seedlings actually exceeded the growth rate in darkness for approximately 3 hr. At this point, inhibition began to develop, and it approached wild-type levels by 4 hr. The data demonstrate that, apart from the initial transient response, phyA exclusively mediates the response to  $R_C$  during the first 3 hr. However, this influence of phyA does not persist. Remarkably well coordinated with the waning of the phyA-dependent phase is the waxing of the phyB-dependent phase; the switchover occurs approximately 3 hr after the onset of irradiation. This pattern is reminiscent of the two genetically separable phases of growth inhibition induced by blue light in *Arabidopsis* hypocotyls, although the response to blue light is considerably faster, as shown in Fig. 1, and it is mediated by blue-specific photoreceptors (7).

The depletion of phyA, caused by light-induced turnover and down-regulation of *PHYA* expression, is a hallmark of this phytochrome type (15), and it raises the possibility that the disappearance of phyA is at least partly responsible for the loss of its influence on growth. The immunoblot in Fig. 2D demonstrates that the level of phyA polypeptide remained similar to that of dark-grown seedlings during the first hour of  $R_C$ , but was abruptly reduced within 3 hr, as similarly reported previously (16). The level of phyB did not change significantly during this

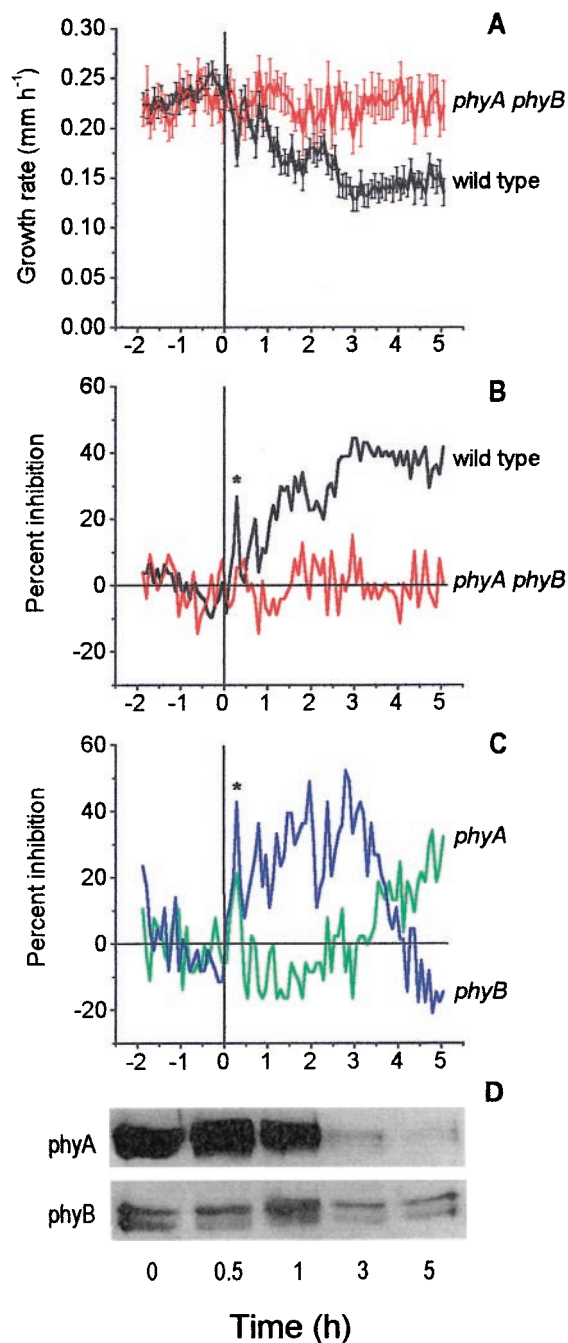


**Fig. 2.** The effect of  $R_C$  on the growth responses and phytochrome levels of *Arabidopsis* seedlings. Seedlings were approximately 3 mm tall for growth rate measurements performed by using CCD image capture. (A) Growth rate data for wild-type and *phyA phyB* double mutant seedlings. Traces shown are the average of 19 and 11 separate measurements for the wild type and the double mutant, respectively. Bars representing 1 SEM are shown at 5-min intervals. (B) Representation of data in A is shown as an inhibition time series, calculated according to Eq. 1 in the text. (C) Inhibition time series showing the averaged responses of 10 *phyA* and 9 *phyB* seedlings to  $R_C$ . For all growth-response curves,  $R_C$  ( $250 \mu\text{mol}\cdot\text{m}^{-2}\cdot\text{s}^{-1}$ ) was initiated at time zero (vertical line). (D) Immunochemically detectable *phyA* and *phyB* in enriched wild-type protein extracts are measured as a function of exposure to  $R_C$  ( $250 \mu\text{mol}\cdot\text{m}^{-2}\cdot\text{s}^{-1}$ ). Each lane was loaded with  $20 \mu\text{g}$  of total protein. The doublet seen on the *phyB* blot probably represents partial degradation of the polypeptide (17). The asterisks shown in B and C denote the early transient phase of growth inhibition. The x-axis labeling at the bottom of the figure applies to all of the panels in this figure.

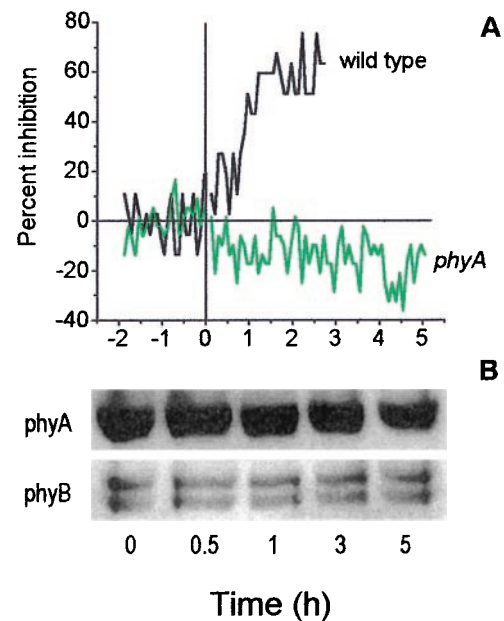


**Fig. 3.** The effect of  $FR_C$  on the growth responses and phytochrome levels of *Arabidopsis* seedlings. Seedlings were approximately 3 mm tall when growth rate measurements were performed by CCD image capture. (A) Growth kinetics of wild-type and *phyA* seedlings in response to  $FR_C$  ( $250 \mu\text{mol}\cdot\text{m}^{-2}\cdot\text{s}^{-1}$ ) are displayed as percentages of the inhibition time series, calculated according to Eq. 1 in the text. Traces are the averages of three and six separate measurements for wild-type and *phyA* seedlings, respectively. (B) Immunochemically detectable *phyA* and *phyB* in enriched wild-type protein extracts, measured as a function of exposure to  $FR_C$  ( $250 \mu\text{mol}\cdot\text{m}^{-2}\cdot\text{s}^{-1}$ ). Each lane was loaded with  $20 \mu\text{g}$  of total protein. The doublet seen on the *phyB* blot probably represents partial degradation of the polypeptide (17). The x-axis labeling at the bottom of the figure applies to both panels.

same light treatment, which is an established feature of this phytochrome type (10, 17). Thus, the loss of the inhibitory influence of *phyA* on growth closely paralleled its disappearance, and was coincident with the onset of the growth control exerted by *phyB*, the level of which remained unchanged throughout the  $R_C$  treatment (Fig. 2D). The increase in the contribution of *phyB* occurred within the reported 2- to 4-hr window when red light causes *phyB* to migrate into the nucleus (18, 19). It is reasonable, then, to suggest that nuclear import of *phyB* may be a prerequisite for its effect on growth.

High-irradiance, continuous far-red light ( $FR_C$ ) strongly inhibits hypocotyl elongation. A kinetic analysis was undertaken to test whether two phytochrome species also contribute to this response, which has usually been attributed to the sole action of *phyA* (5). The inhibition time series of wild-type and *phyA* seedlings exposed to  $FR_C$  are compared in Fig. 3A. The wild-type response to  $FR_C$  was robust, greater than that induced by  $R_C$ , and it lacked an initial transient phase. Consistent with the long-hypocotyl phenotype of *phyA* seedlings observed after days of growth in  $FR_C$  (20–22), no inhibition could be detected in the *phyA* seedlings. Even increasing the far-red fluence rate to  $1600 \mu\text{mol}\cdot\text{m}^{-2}\cdot\text{s}^{-1}$  did not induce a detectable response in *phyA* seedlings (data not shown). In fact, *phyA* seedlings grew considerably faster than in darkness during 5 hr of  $FR_C$ , for reasons that are not understood. Thus, the response to  $FR_C$  appears to be mediated exclusively by *phyA*, at least during the first 5 hr of irradiation. The persistence of *phyA* action in the response to  $FR_C$  is in distinct contrast to its transient influence in  $R_C$ . The immunoblots in Fig. 3B reveal that the level of *phyA* did not change during the 5 hr of  $FR_C$ , which is consistent with the

**Table 1. Fluence dependence of net inhibition, relative to growth in darkness during 5 hr of red light**

Fluence rate, $\mu\text{mol}\cdot\text{m}^{-2}\cdot\text{s}^{-1}$	Inhibition, %		
	Wild type	<i>phyA</i>	<i>phyB</i>
2.5	14.9	3.0	7.5
25	23.8	9.5	12.1
250	28.6	2.7	17.7

persistence of its inhibitory effect on growth. As expected, the levels of *phyB* also did not change (Fig. 3B).

The inhibition time series revealed temporal aspects of phytochrome action, but it was also useful for quantifying the contributions to growth inhibition of specific phytochromes. By numerically integrating Eq. 1 from  $t = 0$  to  $t = 5$  hr (with software), an inhibition index ( $I$ ) was obtained.

$$I = \int_0^{5 \text{ hr}} \left(1 - \frac{r(t)}{r_0}\right) dt. \quad [2]$$

Dividing the value of  $I$  by the duration of the light treatment yielded the net inhibition relative to growth in darkness. Periods in which growth was slower than the average rate in darkness add to the value of the integral, whereas periods of growth in excess of the dark rate subtract from it. The results of this analysis at three  $R_C$  fluence rates are shown in Table 1 for wild-type, *phyA*, and *phyB* seedlings. Increasing the fluence rate of  $R_C$  from 2.5 to 25  $\mu\text{mol}\cdot\text{m}^{-2}\cdot\text{s}^{-1}$  increased the net inhibition in wild-type seedlings, and increasing it to 250  $\mu\text{mol}\cdot\text{m}^{-2}\cdot\text{s}^{-1}$  had a further, though smaller, effect. A separate analysis of the initial transient response indicated that it was already saturated at 2.5  $\mu\text{mol}\cdot\text{m}^{-2}\cdot\text{s}^{-1}$  (data not shown). The sum of the *phyA* and *phyB* contributions ranged from 70% to 91% of the wild-type value over the tested fluence range. The agreement was best at 25  $\mu\text{mol}\cdot\text{m}^{-2}\cdot\text{s}^{-1}$ , which may be related to the fact that *phyA* and *phyB* seedlings did not display periods of growth in excess of the dark rate at this fluence rate of  $R_C$  (data not shown). It is not known what caused the *phyA* and *phyB* seedlings to grow faster in higher fluence light than in darkness (Figs. 2C and 3A). However, the absence of this effect on growth rate in  $R_C$  for *phyA* *phyB* seedlings (Fig. 2A and B) indicates that (i) phytochrome is necessary for this enhanced growth rate, and (ii) *phyA* and *phyB* exhibit functional overlap for this effect, which is observable only when an inhibitory influence on growth by *phyA* or *phyB* is missing because of a deficiency in either of the photoreceptors. Genetic evidence currently supports the existence of a negative regulator of growth (*SPA1*) that requires *phyA* (23), and the data presented here (Fig. 2C) indicate that another such factor requiring *phyB* may also exist, a factor that is inducible by *phyB*.

The hallmark long-hypocotyl phenotype of *phyB*, when grown for several days under  $R_C$ , a situation in which *phyA* contributes much less to hypocotyl inhibition (24), has fostered the view that  $R_C$  acts primarily through *phyB* to inhibit growth (10, 25). However, the analysis presented here demonstrates that *phyA* initiated this response to  $R_C$  (ignoring for the moment the initial

transient inhibition), and prevailed as the primary photoreceptor for the first 3 hr of irradiation. The initiating role of *phyA* shown here and the recent demonstration that the nuclear import of *phyA* is fast [occurring within minutes of red light treatment (18)], may not be a coincidence. As in the case of *phyB*, nuclear import of *phyA* roughly coincides with the onset of its influence on growth.

Only after *phyA* began to disappear and lose influence on growth did *phyB* begin to exert control. This tightly coordinated transition from a *phyA*-dependent mechanism to a *phyB*-dependent mechanism is perhaps the most salient result of the present kinetic analysis. How is this coordination achieved? The recent elegant discoveries of signaling proteins that interact with the carboxyl termini of either *phyA* or *phyB* may provide clues. *PKS1* is a cytoplasmic protein whose sequence gives few clues about its function, although it does act as a substrate *in vitro* and *in vivo* for the kinase activity of phytochrome (26). *PIF3* is found in the nucleus and is a potential transcriptional regulator (27). Perhaps phytochromes initiate signaling only when bound to one or more of these interacting proteins, which may be predominantly associated with *phyA* before irradiation because of its relative abundance. As *phyA* levels decrease in response to  $R_C$ , more complexes involving *phyB* would form, caused by a shift in the relative abundance of *phyB*.

Such competitive binding of a limiting transduction component, coupled with the light-induced decrease in *phyA*, could be a factor in coordinating the transition between *phyA*- and *phyB*-dependent phases of growth control. However, the situation is demonstrably more complicated. Mutants lacking *phyA*, but possessing a normal complement of *phyB* and interacting proteins, would be expected to display an immediate *phyB*-dependent phase of inhibition in response to  $R_C$ , but such a response was not observed (Fig. 2C). And it is important to reemphasize that, in addition to causing growth inhibition, *phyA* also induces *SPA1*, which acts as a negative regulator of growth (23). Studies of *SPA1* have shown it to be induced by  $R_C$  with a time course remarkably similar to the time course of *phyA* action on growth. Therefore, the sequential shift in photocontrol from *phyA* to *phyB* in  $R_C$ , as observed here, may have as much to do with significant alterations of the downstream transduction machinery as with the dynamic changes in photoreceptor levels. A complete description of phytochrome signaling must also take into account the genetic evidence that some downstream molecules are specific for particular phytochromes (6, 16). This amount of complexity is daunting, but high-resolution measurements of physiological processes such as growth promise to add important information. When combined with modern forward and reverse genetics, this approach may be expected to advance our understanding of the complex array of photoreceptor types and transduction elements that bring about photomorphogenesis.

We thank Daniel Lewis for his assistance in these experiments. This work was supported by a grant from the National Aeronautics and Space Administration/National Science Foundation Network for Research on Plant Sensory Systems (IBN-9416016); a grant from the Department of Energy/National Science Foundation/U.S. Department of Agriculture Collaborative Program on Research in Plant Biology to the University of Wisconsin (BIR 92-20331); and a grant from the U.S. Department of Agriculture (99-01833).

1. Yeh, K.-C. & Lagarias, J. C. (1998) *Proc. Natl. Acad. Sci. USA* **95**, 13976–13981.
2. Kendrick, R. E. & Kronenberg, G. H. M., eds. (1994) *Photomorphogenesis in Plants* (Kluwer Academic, Dordrecht, The Netherlands), 2nd Ed.
3. Whitelam, G. C., Patel, S. & Devlin, P. F. (1998) *Philos. Trans. R. Soc. London B* **353**, 1445–1453.
4. Smith, H. (1995) *Annu. Rev. Plant Physiol. Plant Mol. Bio.* **46**, 289–315.
5. Quail, P. H., Boylan, M. T., Parks, B. M., Short, T. W., Xu, Y. & Wagner, D. (1995) *Science* **268**, 675–680.
6. Quail, P. H. (1998) *Philos. Trans. R. Soc. London B* **353**, 1399–1403.

7. Parks, B. M., Cho, M. H. & Spalding, E. P. (1998) *Plant Physiol.* **118**, 609–615.
8. Devlin, P. F., Robson, P. R. H., Patel, S. R., Goosey, L., Sharrock, R. A. & Whitelam, G. C. (1999) *Plant Physiol.* **119**, 909–915.
9. Spalding, E. P. (1995) *Photochem. Photobiol.* **62**, 934–939.
10. Somers, D. E., Sharrock, R. A., Tepperman, J. M. & Quail, P. H. (1991) *Plant Cell* **3**, 1263–1274.
11. Cosgrove, D. J. (1982) *Plant Sci. Lett.* **25**, 305–312.
12. Gaba, V. & Black, M. (1979) *Nature (London)* **278**, 51–54.
13. Meijer, G. (1968) *Acta Bot. Neerl.* **17**, 9–14.

14. Koornneef, M., Rolf, E. & Spruit, C. J. P. (1980) *Z. Pflanzenphysiol.* **100**, 147–160.
15. Clough, R. C. & Vierstra, R. D. (1997) *Plant Cell Environ.* **20**, 713–721.
16. Hudson, M., Ringli, C., Boylan, M. T. & Quail, P. H. (1999) *Genes Dev.* **13**, 2017–2027.
17. Hirschfield, M., Tepperman, J. M., Clack, T., Quail, P. H. & Sharrock, R. A. (1998) *Genetics* **149**, 523–535.
18. Kircher, S., Kozma-Bognar, L., Kim, L., Adams, E., Harter, K., Schäfer, E. & Nagy, F. (1999) *Plant Cell* **11**, 1445–1456.
19. Yamaguchi, R., Nakamura, M., Mochizuki, N., Kay, S. A. & Nagatani, A. (1999) *J. Cell Biol.* **145**, 437–445.
20. Nagatani, A., Reed, J. W. & Chory, J. (1993) *Plant Physiol.* **102**, 269–277.
21. Parks, B. M. & Quail, P. H. (1993) *Plant Cell* **5**, 39–48.
22. Whitelam, G. C., Johnson, E., Peng, J., Carol, P., Anderson, M. L., Cowl, J. S. & Harberd, N. P. (1993) *Plant Cell* **5**, 757–768.
23. Hoecker, U., Tepperman, J. M. & Quail, P. H. (1999) *Science* **284**, 496–499.
24. Mazzella, M. A., Alconada-Magliano, T. M. & Casal, J. J. (1997) *Plant Cell Environ.* **20**, 261–267.
25. Reed, J. W., Nagpal, P., Poole, D. S., Furuya, M. & Chory, J. (1993) *Plant Cell* **5**, 147–157.
26. Fankhauser, C., Yeh, K.-C., Lagarias, J. C., Zhang, H., Elich, T. D. & Chory, J. (1999) *Science* **284**, 1539–1541.
27. Ni, M., Tepperman, J. M. & Quail, P. H. (1998) *Cell* **95**, 657–667.